

Kinetic Investigations Provide Additional Evidence That an Enzyme-like Binding Pocket Is Crucial for High Enantioselectivity in the Bis-Cinchona Alkaloid Catalyzed Asymmetric Dihydroxylation of Olefins

E. J. Corey* and Mark C. Noe

Contribution from the Department of Chemistry, Harvard University, Cambridge, Massachusetts 02138

Received July 31, 1995[⊗]

Abstract: The Sharpless enantioselective dihydroxylation of terminal olefins by OsO₄ using the catalytic chiral ligand (DHQD)₂PYDZ (**1**) has been shown to follow Michaelis–Menten kinetics, demonstrating fast reversible formation of a complex of olefin, OsO₄, and **1** prior to the rate-limiting conversion to the Os(VI) ester intermediate. There is a good correlation between the observed binding constants, K_m , and the degree of enantioselectivity of the dihydroxylation indicating that van der Waals binding of the substrate by **1**•OsO₄ is important to enantioselective rate enhancement. Inhibition of the oxidation by various compounds has been demonstrated kinetically using Dixon analysis of the data, and K_i values have been determined and correlated with inhibitor structure. The strongest inhibitors are compounds with the ability to coordinate to Os(VIII) of the **1**•OsO₄ complex while simultaneously binding in the pocket formed by the aromatic subunits of the ligand. Parallelism between K_m and K_i values and their relationship with structure indicate similar binding in the substrate and inhibitor complexes with **1**•OsO₄. The kinetic, structural, and stereochemical data, as summarized in Tables 1 and 3, support a mechanism for the enantioselective dihydroxylation which involves (1) rapid, reversible formation of an olefin–Os(VIII) π -d complex and (2) slow rearrangement to the [3 + 2] cycloaddition transition state which is exemplified in Figure 12. In terms of this mechanism, enantioselective acceleration is the result of two factors: (1) enzyme–substrate-like complexation which brings the reactants together in the appropriate geometry for further conversion to the predominating enantiomer, thereby providing a high effective reactant concentration (entropic effect) and (2) a driving force in the next step due to relief of eclipsing strain about the OsO₄–N bond which lowers the activation enthalpy. Taken together with existing data on the Sharpless enantioselective dihydroxylation, the present results strongly support the [3 + 2] cycloaddition pathway and the U-shaped binding pocket which was advanced earlier.

Introduction

Starting from the initial observation that dihydroquinidine acetate catalyzes the OsO₄-promoted dihydroxylation of olefins and produces 1,2-diols with modest enantioselectivity, for example $R/S = ca. 4$ for styrene,¹ Sharpless and co-workers screened many other derivatives of dihydroquinidine with gradual improvement of enantioselectivity.² The highest enantioselectivities were observed with bis-cinchona alkaloid derivatives of the type shown in formula **1** ($R/S = 32$). For some time, we have been studying the mechanistic basis for enantioselectivity in the OsO₄-promoted dihydroxylation of olefins using bis-cinchona alkaloids such as **1** as catalysts.³ This work has led to the proposal of a transition-state model which can be summarized by formula **3** for the specific case of allyl 4-methoxybenzoate (**2**) as substrate and the pyridazine-linked bis-dihydroquinidine derivative **1** ((DHQD)₂PYDZ). This transition state and the mechanistic pathway have the following characteristics: (1) a preference for the U-shaped conformation as in **3** for the OsO₄ complex, which has the ability to hold olefinic

substrates such as **2** in a binding pocket composed of the two parallel methoxyquinoline units, OsO₄ and the pyridazine connector, as shown, (2) staggered geometry about the Os–N bond of the bis-cinchona–OsO₄ complex, (3) the proximity of one axial oxygen (O_a) and one equatorial oxygen (O_e) of the complexed OsO₄ unit to the olefinic carbons of the bound substrate, as shown, and (4) a minimum motion pathway from this arrangement for the [3 + 2] cycloaddition which directly produces the pentacoordinate osmate ester in the energetically most favorable geometry. The rate acceleration for the observed enantioselective pathway relative to other modes is due to the favorable free energy of activation for the reaction from the complex **3** in which the reactants are held in a manner which is ideal for the formation of the thermodynamically more stable osmate ester. Dihydroxylation of the opposite olefin face to that shown in **3** is unfavorable due to the fact that there is no three-dimensional arrangement for simultaneous π -facial approach of the olefin to the oxygens labeled as O_a and O_e and favorable interaction with the binding pocket.⁴ X-ray crystallographic data suggest that the pyridazine ring at the bottom of the U-shaped cavity tends to be oriented so as to allow conjugation of the ring and the two alkoxy substituents, with the N–N side of the ring participating in binding to the substrate, though the exact tilt of this ring during reaction probably varies

[⊗] Abstract published in *Advance ACS Abstracts*, December 15, 1995.

(1) Hentges, S. G.; Sharpless, K. B. *J. Am. Chem. Soc.* **1980**, *102*, 4263.

(2) For a recent review of the development and applications of the Sharpless asymmetric dihydroxylation, see: Kolb, H. C.; VanNieuwenhze, M. S.; Sharpless, K. B. *Chem. Rev.* **1994**, *94*, 2483.

(3) (a) Corey, E. J.; Noe, M. C.; Sarshar, S. *J. Am. Chem. Soc.* **1993**, *115*, 3828. (b) Corey, E. J.; Noe, M. C. *J. Am. Chem. Soc.* **1993**, *115*, 12579. (c) Corey, E. J.; Noe, M. C.; Sarshar, S. *Tetrahedron Lett.* **1994**, *35*, 2861. (d) Corey, E. J.; Noe, M. C.; Grogan, M. J. *Tetrahedron Lett.* **1994**, *35*, 6427.

(4) (a) Corey, E. J.; Guzman-Perez, A.; Noe, M. C. *J. Am. Chem. Soc.* **1994**, *116*, 12109. (b) Corey, E. J.; Guzman-Perez, A.; Noe, M. C. *J. Am. Chem. Soc.* **1995**, *117*, 10805. (c) Corey, E. J.; Noe, M. C.; Guzman-Perez, A. *J. Am. Chem. Soc.* **1995**, *117*, 10817.

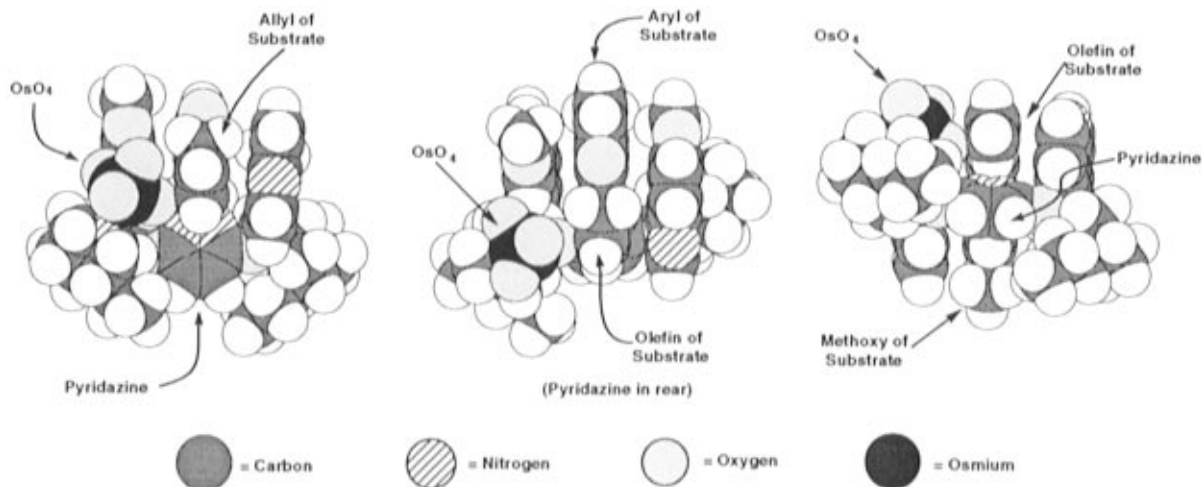


Figure 1. Three views of the proposed transition-state assembly for the dihydroxylation of **2**.

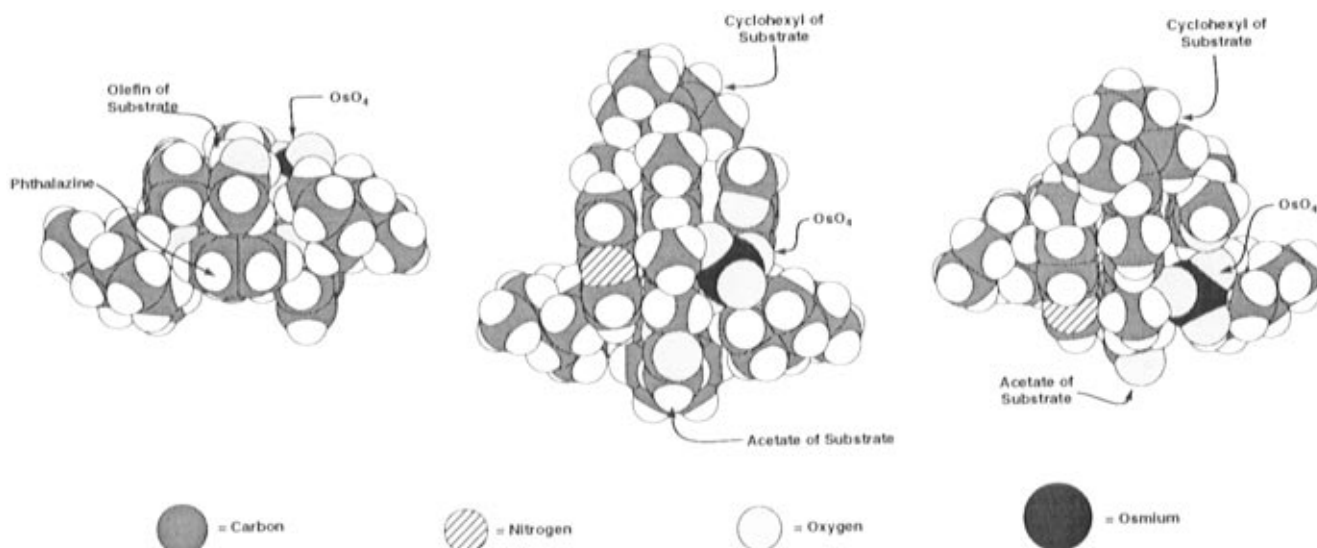
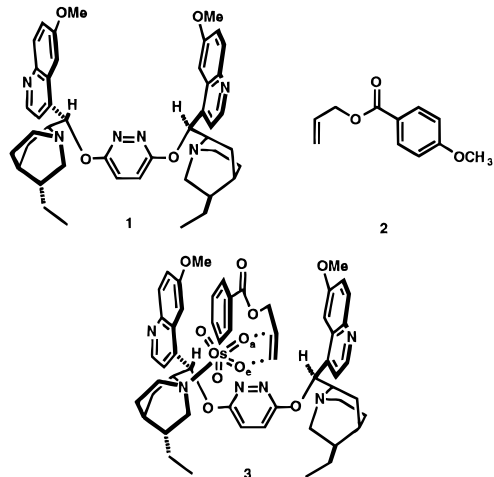


Figure 2. Three views of the proposed transition-state assembly for the dihydroxylation of **4**.

slightly with substrate.^{3c} When allyl 4-methoxybenzoate is used as reactant, excellent binding of this substrate can be expected because of extensive π -contact of both faces of the allyl and 4-methoxybenzoate moieties with the two methoxyquinoline units and edge contact with the pyridazine ring.^{4b,c}



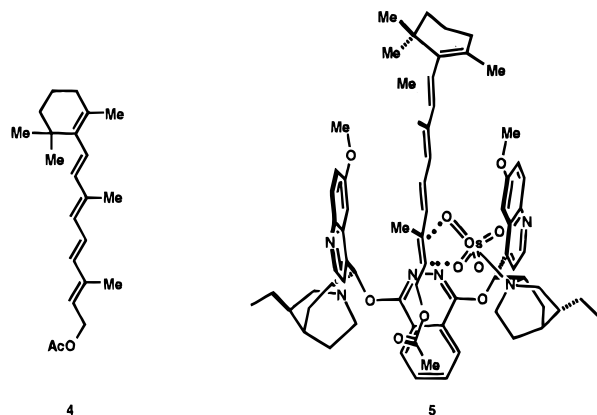
Three views of transition state **3** using a space-filling representation are shown in Figure 1. The complementary shapes and the potential for binding between the catalyst and

substrate which are apparent from Figure 1 suggest the possibility of a reversibly formed complex of catalyst and substrate which might precede transition state development in a manner paralleling reversibly formed enzyme–substrate complexes. It became apparent from these considerations that kinetic studies of the dihydroxylation of appropriate substrates might reveal the existence of such an intermediate by the appearance of Michaelis–Menten behavior.⁵

The transition state model described above accommodates all of the experimental facts of which we are aware. In addition, it has also been of great predictive value. For instance, the model predicted the possibility of position and enantioselective dihydroxylation of retinyl acetate (**4**) at the 2,3-double bond. This result was demonstrated experimentally and applied to a successful and simple synthesis of the signaling retinoid (14*R*)-14-hydroxy-4,14-retro-retinol via transition state **5**; see also Figure 2.⁶

(5) Detailed kinetic studies of the stoichiometric reactions of various cinchona alkaloid- OsO_4 catalysts with several olefins have been carried out by Sharpless and co-workers. See: (a) Andersson, P. G.; Sharpless, K. B. *J. Am. Chem. Soc.* **1993**, *115*, 7047. (b) Kolb, H. C.; Andersson, P. G.; Bennani, Y. L.; Crispino, G. A.; Jeong, K.-S.; Kwong, H.-L.; Sharpless, K. B. *J. Am. Chem. Soc.* **1993**, *115*, 12226. (c) Kolb, H. C.; Andersson, P. G.; Sharpless, K. B. *J. Am. Chem. Soc.* **1994**, *116*, 1278.

(6) Corey, E. J.; Noe, M. C.; Guzman-Perez, A. *Tetrahedron Lett.* **1995**, *36*, 4171.



Results and Discussion

The first positive indication that Michaelis–Menten kinetic behavior might be exhibited in the bis-cinchona alkaloid catalyzed dihydroxylation of olefins was obtained from a set of competition experiments involving allyl 4-methoxybenzoate (**2**) and allyl triisopropylsilyl ether (**6**). These substrates were selected for initial studies due to the large differences in their reactivity with the $(\text{DHQD})_2\text{PYDZ}\cdot\text{OsO}_4$ catalyst ($\mathbf{1}\cdot\text{OsO}_4$) that were anticipated from application of the transition state model depicted in Figure 1. Stabilizing aryl–aryl interactions between the allylic 4-methoxybenzoate group of **2** within the U-shaped binding pocket of the $(\text{DHQD})_2\text{PYDZ}\cdot\text{OsO}_4$ catalyst ($\mathbf{1}\cdot\text{OsO}_4$) should accelerate the overall reaction rate of this substrate relative to that of **6** which cannot effectively bind to the catalyst due to the large steric demand of the allylic triisopropylsilyloxy group. The catalytic asymmetric dihydroxylation of a 1:1 mixture of these substrates was followed by gas chromatographic analysis using tetralin as an internal standard. The conversion of each substrate as a function of total reaction time is indicated in Figure 3. As shown, the $(\text{DHQD})_2\text{PYDZ}\cdot\text{OsO}_4$ catalyst ($\mathbf{1}\cdot\text{OsO}_4$) selectively dihydroxylates allyl 4-methoxybenzoate (**2**) before beginning to react with allyl triisopropylsilyl ether (**6**). Only trace amounts of **6** react during the first 80% of the reaction of **2**, and the calculated ratio of the dihydroxylation rates for these substrates during this period is $>50:1$. Allyl triisopropylsilyl ether (**6**) begins to react at a more rapid rate only after most of the allyl 4-methoxybenzoate **2** is consumed. The absence of an induction period in the independent reaction of allyl triisopropylsilyl ether (**6**) was verified by a control experiment in the absence of substrate **2**. In this case, the intrinsic rate of reaction of **2** was approximately six-fold faster than that of **6**.⁷

The observation of inhibition of the dihydroxylation of allyl triisopropylsilyl ether (**6**) in the presence of allyl 4-methoxybenzoate (**2**) is readily explained in terms of a substrate–catalyst binding equilibrium that exists prior to transition state development in the asymmetric dihydroxylation. According to this model, both substrates **2** and **6** compete for a single active binding site on the bis-cinchona alkaloid catalyst $\mathbf{1}\cdot\text{OsO}_4$. Substrate **2** binds more tightly (lower K_m) due to the favorable aryl–aryl stacking and other van der Waals interactions with the catalyst relative to substrate **6**, which cannot fit well into the catalyst binding cleft due to unfavorable steric repulsions involving the bulky triisopropylsilyloxy group. In the presence of a low, substoichiometric amount of **1** (ca. 1 mol % based on total olefin), nearly all of the catalyst will be associated with **2**

(7) Rates of reaction refer to initial velocities during the first 5–20% of the reaction of any given substrate. Concentrations refer to the organic layer (ca. 2:1 *t*-BuOH:H₂O) and were shown by GC and UV analysis to be within 5% of the calculated values.

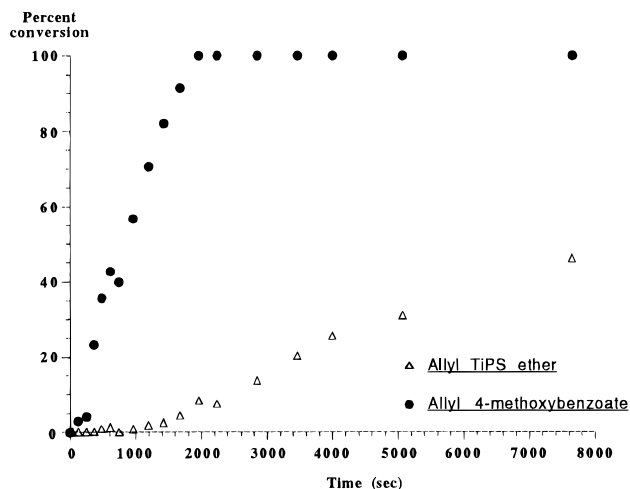


Figure 3. Reaction profile for the competitive catalytic asymmetric dihydroxylation of allyl 4-methoxybenzoate (**2**) (0.08 M) and allyl triisopropylsilyl ether (**6**) (0.08 M) using the $(\text{DHQD})_2\text{PYDZ}$ ligand **1** (1.6 mM) and $\text{K}_2\text{OsO}_4\cdot 2\text{H}_2\text{O}$ (0.4 mM) in 1:1 *tert*-butyl alcohol–H₂O at 0 °C.

during the initial stages of the reaction, and the reaction of **6** will be suppressed. As **2** is consumed, the amount of free catalyst $\mathbf{1}\cdot\text{OsO}_4$ increases, and the oxidation of **6** proceeds at a more rapid rate. Such kinetic behavior has been observed for several enzymatic reactions, and a theoretical treatment has been derived.⁸

Similar reactivity was observed in the competitive asymmetric dihydroxylation of 4-vinylanisole (**8**) vs 1-decene (**10**) and 4-vinylanisole (**8**) vs allyl triisopropylsilyl ether (**6**). In each case, the substrate that exhibits higher enantioselectivity in the corresponding independent dihydroxylation reaction is also that which suppresses the dihydroxylation of the other olefin. Moreover, the degree of suppression reflects the difference in enantioselectivities in the dihydroxylation reaction and in binding affinities of the two substrates to the catalyst $\mathbf{1}\cdot\text{OsO}_4$ (*vide infra*). Thus, vinylanisole partially suppresses the dihydroxylation of 1-decene and allyl triisopropylsilyl ether but has little effect on the dihydroxylation of styrene using the $(\text{DHQD})_2\text{PYDZ}\cdot\text{OsO}_4$ catalyst, $\mathbf{1}\cdot\text{OsO}_4$, as shown in Figures 4–6, respectively.

More detailed studies were undertaken in order to further examine the relationships between catalyst and substrate structure, binding, and enantioselectivity in the catalytic asymmetric dihydroxylation reaction using Michaelis–Menten analysis. Such a study of the catalytic reaction requires that the following conditions hold: (1) catalyst and substrate react reversibly to form a complex; (2) the equilibrium association and dissociation rates for the catalyst–substrate complex are rapid relative to the rate of formation of the osmate ester intermediate; (3) the catalyst concentration is small, such that formation of the catalyst–substrate complex does not alter the total substrate concentration; (4) the overall reaction rate is limited by the conversion of the catalyst–substrate complex to the osmate ester intermediate and not by subsequent steps of the catalytic cycle; and (5) the velocity is measured during the initial stages of the

(8) For examples of this phenomenon in biological systems, see: (a) Hackette, S. L.; Skye, G. E.; Burton, C.; Segel, I. H. *J. Biol. Chem.* **1970**, *245*, 4241. (b) Dixon, M.; Webb, E. C. *Enzymes*, 2nd ed.; Chapter 4, p 88. For another example observed by Willstatter, R.; Kuhn, R.; Lind, O.; Memmen, F. Z. *Physiol. Chem.* **1927**, *167*, 303. For theoretical treatments of kinetic behavior observed in cases of mutual competitive inhibition, see: (c) Pocklington, T.; Jeffery, J. *Biochem. J.* **1969**, *112*, 331. (d) Dixon, M.; Webb, E. C. *Enzymes*, 2nd ed.; Chapter 4, pp 84–87.

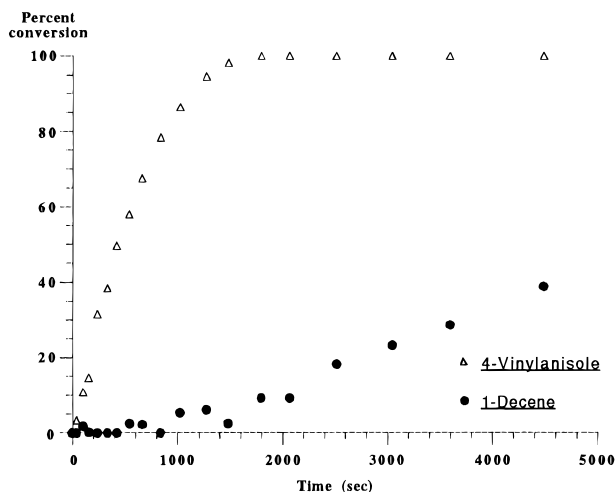


Figure 4. Reaction profile for the competitive catalytic asymmetric dihydroxylation of decene (0.08 M) and 4-vinyl anisole (0.08 M) using (DHQD)₂PYDZ ligand **1** (1.6 mM) and K₂OsO₄·2H₂O (0.4 mM) in 1:1 *tert*-butyl alcohol–H₂O at 0 °C.

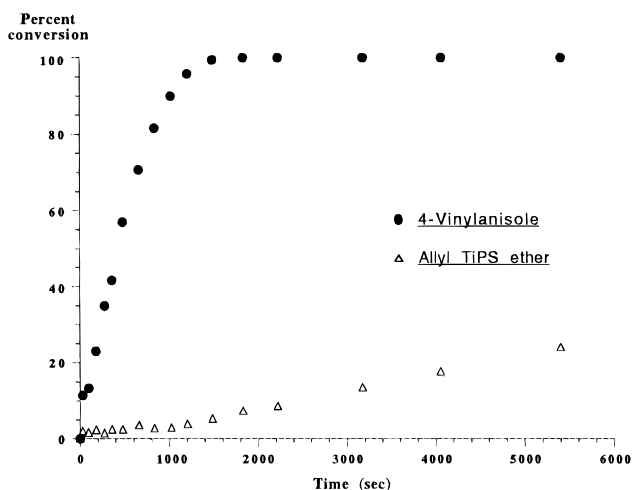


Figure 5. Reaction profile for the competitive catalytic asymmetric dihydroxylation of allyl triisopropylsilyl ether (0.08 M) and 4-vinyl-anisole (0.08 M) using (DHQD)₂PYDZ ligand **1** (1.6 mM) and K₂OsO₄·2H₂O (0.4 mM) in 1:1 *tert*-butyl alcohol–H₂O at 0 °C.

reaction.⁹ Assumptions (1) and (2) are clearly valid since the catalyst possesses one binding site for the substrate, and since association and dissociation of the substrate with the U-shaped binding pocket should be very rapid compared to cycloaddition to form the osmate ester. Assumptions (3) and (5) can be assured by an appropriate experimental design. Assumption (4) is valid only if the steps to regenerate the catalyst from the osmate ester intermediate are rapid relative to its formation.¹⁰

The sequence of events in the catalytic asymmetric dihydroxylation reaction using the K₃Fe(CN)₆ secondary oxidant system has previously been demonstrated.¹¹ The reaction mixture is triphasic, consisting of a solid phase of undissolved salts, a salt-containing aqueous phase, and an organic phase consisting of the ligand, substrate, and catalyst-bound osmium tetroxide in *ca.* 2:1 *tert*-butyl alcohol–water (ratio determined by us using both ¹H NMR and density measurements on the vacuum-transferred liquid). The first irreversible step in the catalytic sequence is oxidation of the olefin by the bis-cinchona alkaloid ligand osmium tetroxide complex to form a pentaco-

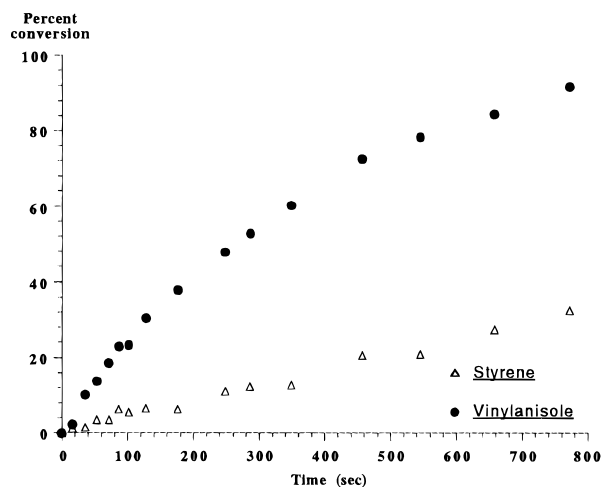
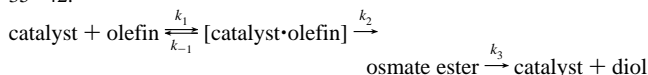


Figure 6. Reaction profile for the competitive catalytic asymmetric dihydroxylation of styrene (0.04 M) and 4-vinyl-anisole (0.04 M) using (DHQD)₂PYDZ ligand **1** (1.0 mM) and K₂OsO₄·2H₂O (0.5 mM) in 1:1 *tert*-butyl alcohol–H₂O at 0 °C.

ordinate osmate ester. This species is subsequently hydrolyzed to produce the diol and OsO₂(OH)₄²⁻. This Os(VI) species then migrates to the aqueous layer, where it is reoxidized by the stoichiometric oxidant K₃Fe(CN)₆ to regenerate OsO₄.^{11c} In cases where the olefin is di-, tri-, or tetrasubstituted, the rate limiting step is the hydrolysis of the osmate ester. However, for most terminal or 1,1-disubstituted substrates, the hydrolysis of the intermediate osmate ester is rapid, and initial attack of the olefin by osmium tetroxide has been found to be rate limiting.¹² The studies reported herein were carried out exclusively with monosubstituted or deactivated 1,2-disubstituted olefins for which addition to the olefin is anticipated to be rate limiting. For the case of styrene careful control studies were carried out which demonstrated that under the conditions of the kinetic studies described herein both the oxidation step, Os(VI) → Os(VIII), and the hydrolysis of cyclic osmate ester to diol are relatively fast compared to the conversion of styrene to the cyclic osmate ester, which therefore is the rate-limiting step. First of all, the rate of oxidation of K₂OsO₂(OH)₄ to Os(VIII) was measured by the stopped-flow method (0.005 M potassium (VI) osmate, 0.08 M K₃Fe(CN)₆, and 0.08 M K₂CO₃ in H₂O at 25 °C) and was found to be very fast with the pseudo-first-order rate constant, *k*₁, determined to be > 100 s⁻¹. This is a much faster reaction than the catalyzed formation of osmate ester from styrene for which *k*₁ has been measured by

(10) For the case where this assumption is invalid, an equation similar to the Henri–Michaelis–Menten equation can be derived using the Briggs–Haldane steady state approach. Thus, $v = V_{\max}[\text{olefin}]/(K_m + [\text{olefin}])$ where $V_{\max} = k_2k_3[\text{catalyst}]_0/(k_2 + k_3)$ and $K_m = [k_3(k_{-1} + k_2)]/(k_2 + k_3 \cdot k_1)$. For these equations, the scheme at the end of the reference applies. Thus, when the complexation–decomplexation equilibrium is fast, *k*₁ and *k*₋₁ ≫ *k*₂. If *k*₂ is rate limiting, then *k*₃ ≫ *k*₂ and $V_{\max} = k_2[\text{catalyst}]_0$ and $K_m = k_{-1}/k_1$, as anticipated for normal Michaelis–Menten behavior. When *k*₃ is rate limiting, *k*₃ ≪ *k*₂, and the same qualitative kinetic behavior is observed, but $V_{\max} = k_3[\text{catalyst}]_0$ and $K_m = (k_{-1}/k_1)(k_3/k_2)$, so the V_{\max} reflects the maximum hydrolysis rate, and the K_m reflects the initial catalyst–substrate equilibrium constant multiplied by a factor of *k*₃/*k*₂. See: Roberts, D. V. *Enzyme Kinetics*; Cambridge University Press: London, 1977; pp 35–42.



(11) (a) Minato, M.; Yamamoto, K.; Tsuji, T. *J. Org. Chem.* **1990**, *55*, 766. (b) Kwong, H.-L.; Sorato, C.; Ogino, Y.; Chen, H.; Sharpless, K. B. *Tetrahedron Lett.* **1990**, *31*, 2999. (c) Ogino, Y.; Chen, H.; Kwong, H.-L.; Sharpless, K. B. *Tetrahedron Lett.* **1991**, *32*, 3965.

(12) Berrisford, D. J.; Bolm, C.; Sharpless, K. B. *Angew. Chem., Int. Ed. Engl.* **1995**, *34*, 1059.

(9) Segel, I. H. *Enzyme Kinetics – Behavior and Analysis of Rapid Equilibrium and Steady-State Enzyme Systems*; John Wiley & Sons, Inc.: New York, 1993; pp 18–22.

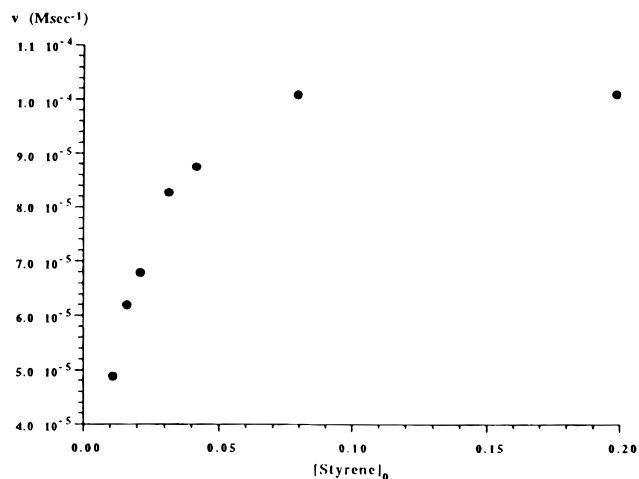


Figure 7. Plot of initial velocity versus initial olefin concentration showing saturation behavior for the (DHQD)₂PYDZ·OsO₄ catalyzed asymmetric dihydroxylation using 1 mM (DHQD)₂PYDZ ligand, 0.5 mM K₂OsO₄·2H₂O in 1:1 *tert*-butyl alcohol–water at 0 °C.

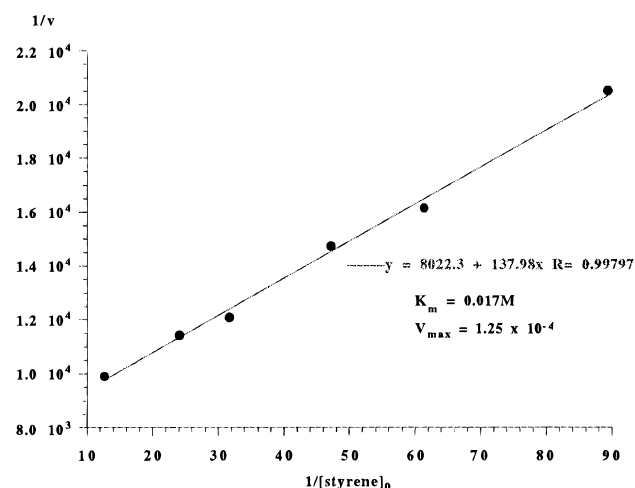


Figure 8. Lineweaver–Burk plot for the catalytic asymmetric dihydroxylation of styrene under the conditions noted in Figure 7.

Sharpless et al.^{5c} (as confirmed by us) to be *ca.* 1 s⁻¹. We have also measured the pseudo-first-order rate constant for hydrolysis of the cyclic osmate ester of styrene under our kinetic conditions (in 0.025 M K₂CO₃ in 2:1 *tert*-butyl alcohol–H₂O at 0 °C) and found *k*₁ to be >200 s⁻¹, i.e., very fast compared to formation of cyclic osmate ester. Similarly, control experiments showed that for the case of methyl cinnamate as substrate, the formation of osmate ester is the rate-limiting step in the catalytic dihydroxylation under the kinetic conditions described herein.

Initial velocities for the reaction of various olefins in the catalytic asymmetric dihydroxylation were measured in order to determine binding constants for these substrates. Reactions were followed by gas chromatographic analysis using an internal standard and were carried out to 10–30% conversion. The (DHQD)₂PYDZ·OsO₄ catalyst displays saturation behavior with respect to olefin concentration, as shown in Figure 7 for the case of styrene. Binding constants for the various olefins were obtained from Lineweaver–Burk plots of 1/velocity vs 1/[substrate]. A representative plot for the case of styrene is shown in Figure 8. A comparison of *K*_m, *V*_{max}, and enantioselectivity values for the olefins tested appears in Table 1. These data were obtained for a fixed concentration of ligand (1 mM) and of OsO₄ (0.5 mM); increasing the concentration of OsO₄ (or ligand) would increase the rate of reaction and, hence, *V*_{max},

Table 1. Comparison of the Michaelis–Menten parameters *K*_m and *V*_{max} and Observed Enantioselectivity in the Catalytic Asymmetric Dihydroxylation of Olefins^a

Entry	Olefin (formula no.)	<i>K</i> _m	<i>V</i> _{max}	% ee
1	(2)	0.017M	1.1 x 10 ⁻⁴	98 ^{4a}
2	(6)	0.49M	5.5 x 10 ⁻⁶	13 ^{4b}
3	(7)	0.017M	1.3 x 10 ⁻⁴	96 ^{3a,b}
4	(8)	0.0068M	6.5 x 10 ^{-5†}	97 [*]
5	(9)	0.0088M	1.0 x 10 ⁻⁴	97 [*]
6	(10)	0.061M	3.8 x 10 ⁻⁶	79 ^{3a,b}
7	(11)	0.0075M	1.7 x 10 ⁻⁶	98 [*]
8	(12)	0.0045M	1.4 x 10 ⁻⁶	98 [*]
9	(7)	0.15M	4.0 x 10 ⁻⁶	40 ^{3a}
DHQD-PYDZ-OMe Ligand (13)				

[†] This reaction was performed using 0.5 mM (DHQD)₂PYDZ ligand and 0.25 mM K₂OsO₄·2H₂O

^{*} This work.

^a Unless otherwise indicated, all reactions were performed at 0 °C in 1:1 *tert*-butyl alcohol–water using the (DHQD)₂PYDZ ligand (1 mM) and K₂OsO₄·2H₂O (0.5 mM).

since at these concentrations significant amounts of free OsO₄ and ligand are present in equilibrium with OsO₄·ligand.^{5c} Thus, the values of *V*_{max} given in Table 1, refer specifically to 1 mM ligand and 0.5 mM OsO₄. However, the *K*_m values shown in Table 1 are independent of the exact concentrations of ligand and OsO₄ within the catalytic range. That follows since *K*_m is equal simply to the substrate concentration at the point where free catalyst and substrate–catalyst concentrations are equal.

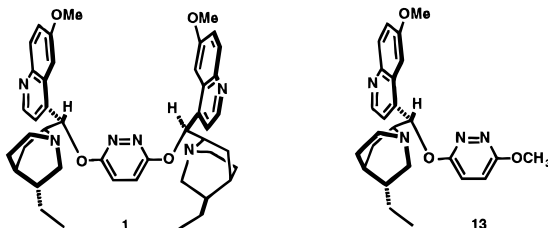
The strong correlation between the binding constants *K*_m and the enantioselectivities observed in the catalytic asymmetric dihydroxylation imply that binding interactions between the catalyst and the substrate are crucial for enantioselection in the dihydroxylation. The structural factors important for binding of the substrate to the catalyst are consistent with those observed earlier for high enantioselectivity in the reaction.³ Olefins that possess hydrophobic substituents of <4 Å thickness, particularly aromatic groups, exhibit the strongest binding affinities and highest enantioselectivities in the reaction, while those substrates which possess bulky groups, such as allyl triisopropylsilyl ether **6**, exhibit weak binding and poor levels of enantioselectivity. These observations suggest that the catalyst imposes steric constraints on the substrates on which it operates that are similar to the substrate requirements of enzymes for activity.^{3b} The lower enantioselectivities observed with substrates **6** and **10** can be understood in terms of competing non-face selective reaction with **1**·OsO₄ without simultaneous binding to the U-shaped pocket, i.e., to other O–Os–O sites. Moreover, alteration of the catalyst binding pocket affects both its ability to bind substrates and the enantioselectivity of the dihydroxylation. Thus, the truncated DHQD-PYDZ-OMe ligand **13** and OsO₄ effect the dihydroxylation of styrene at a slower rate and with much lower enantioselectivity than is observed for the corre-

Table 2. Observed and Calculated Initial Velocity Ratios (Φ) for Multiple Substrate Competition Experiments^a

substrate combination	calcd Φ	obsd Φ
styrene—decene	12.3	8.6
decene—allyl TiPS ether	5.5	5.6
4-vinylanisole—styrene	5.0	4.2
4-vinylanisole—4-CN styrene	3.4	3.4

^a All reactions were run with 0.04 M initial substrate concentration using 1 mM (DHQD)₂PYDZ ligand and 0.5 mM K₂OsO₄·2H₂O at 0 °C in 1:1 *tert*-butyl alcohol—water. The faster reacting olefin is indicated first.

sponding reaction of ligand **1** and OsO₄,^{3a} a consequence of the much diminished binding capacity of **13**·OsO₄ with styrene.¹³



In order to confirm the validity of the observed catalytic parameters K_m and V_{max} , ratios of initial velocities for a few representative substrates were independently determined by competition studies and compared with the values from Michaelis—Menten analysis.¹⁴ As indicated in Table 2, the observed ratio of rates, Φ , agrees with the corresponding ratio calculated from the above Michaelis—Menten parameters for each olefin combination tested.

Since the ratio of initial velocities for the dihydroxylation of two competing substrates is dictated by the corresponding ratio of rates for the first irreversible step in the catalytic dihydroxylation, the good agreement between the observed and calculated ratios Φ provides further support that, for the cases tested above, the rate limiting step in the catalytic sequence is the initial oxidation of the substrate double bond and not the subsequent breakdown of the corresponding osmate ester and also confirms the reliability of the observed values of K_m and V_{max} .

Additional evidence for a catalyst—substrate complex intermediate was also obtained from competitive inhibition studies involving rationally designed olefinic and non-olefinic inhibitors. The catalytic asymmetric dihydroxylation of styrene by the (DHQD)₂PYDZ·OsO₄ complex was studied in the presence of several inhibitors with the results shown in Table 3. In each case, the inhibition constant K_i was determined from a linear Dixon plot of $1/v$ vs inhibitor concentration, [inhibitor], at an initial substrate concentration of K_m . Two representative examples are shown in Figures 9 and 10. The observation of linear competitive inhibition indicates that the substrate and the inhibitor compete for association with the same catalyst binding site.

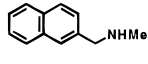
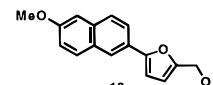
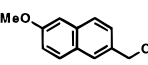
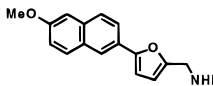
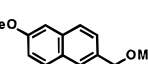
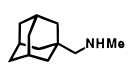
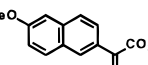
(13) While the ratio of V_{max} for the corresponding catalysts **1**·OsO₄ and **13**·OsO₄ is only 3:1, the ratio of rates for the catalytic dihydroxylation of styrene involving an equimolar mixture of **1** and **13** will vary between 8:1 and 30:1 at [styrene]₀ = 80 mM depending on the extent of conversion according to the formula

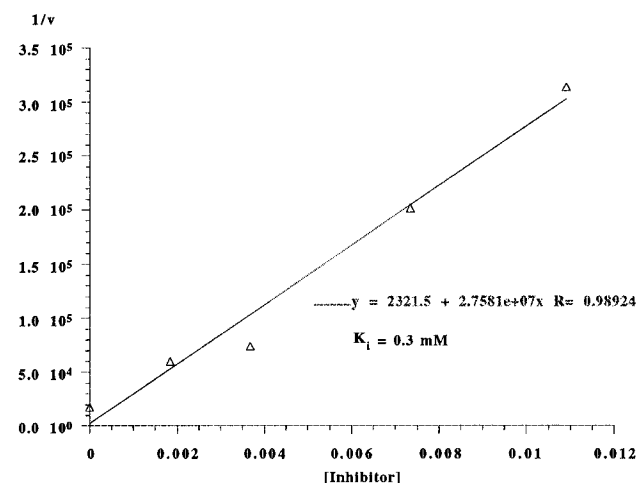
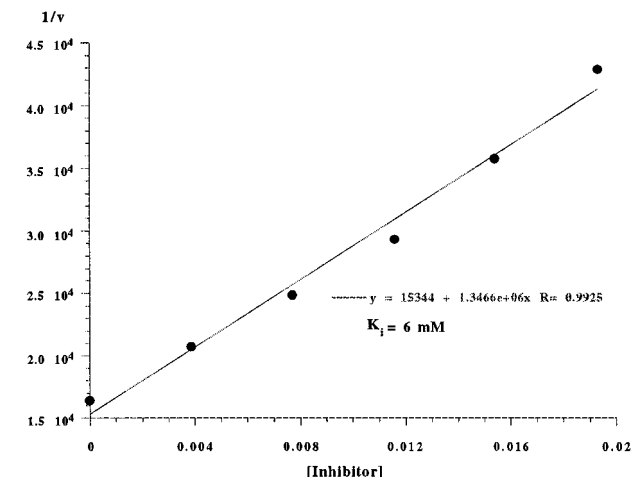
$$\frac{v_1}{v_2} = \frac{V_{max1}(K_{m2} + [\text{olefin}])}{V_{max2}(K_{m1} + [\text{olefin}])}$$

(14) The theoretical value for the ratio of initial rates in the competitive reaction of two substrates at equimolar initial concentrations with a single enzyme is given by Φ (see equation at end of reference) and $V_A = V_{max}$ for substrate A, $V_B = V_{max}$ for substrate B, $K_A = K_m$ for substrate A and $K_B = K_m$ for substrate B

$$\Phi = \frac{V_A K_B}{V_B K_A}$$

Table 3. Inhibition of the Catalytic Asymmetric Dihydroxylation of Styrene Using the (DHQD)₂PYDZ·OsO₄ Catalyst **1**·OsO₄

Inhibitor	K_i	Inhibitor	K_i
	1.6 mM		6.0 mM
	27 mM		0.30 mM
	71 mM		26 mM
	1.2 mM		

**Figure 9.** Dixon plot for the inhibition of the asymmetric dihydroxylation of styrene using the (DHQD)₂PYDZ·OsO₄ catalyst by **19**. The initial styrene concentration was 17.5 mM. The reaction conditions are the same as those detailed in Figure 7.**Figure 10.** Dixon plot for the inhibition of the asymmetric dihydroxylation of styrene using the (DHQD)₂PYDZ·OsO₄ catalyst by **18**. The initial styrene concentration was 17.5 mM. The reaction conditions are the same as those detailed in Figure 7.

In each case, the strongest inhibition of catalytic activity was observed for structures possessing two binding groups: a hydrophobic aromatic group which binds in the catalyst U-shaped binding pocket and a hydroxyl or amine function which can coordinate with osmium (VIII). Thus, *N*-methylnaphtha-

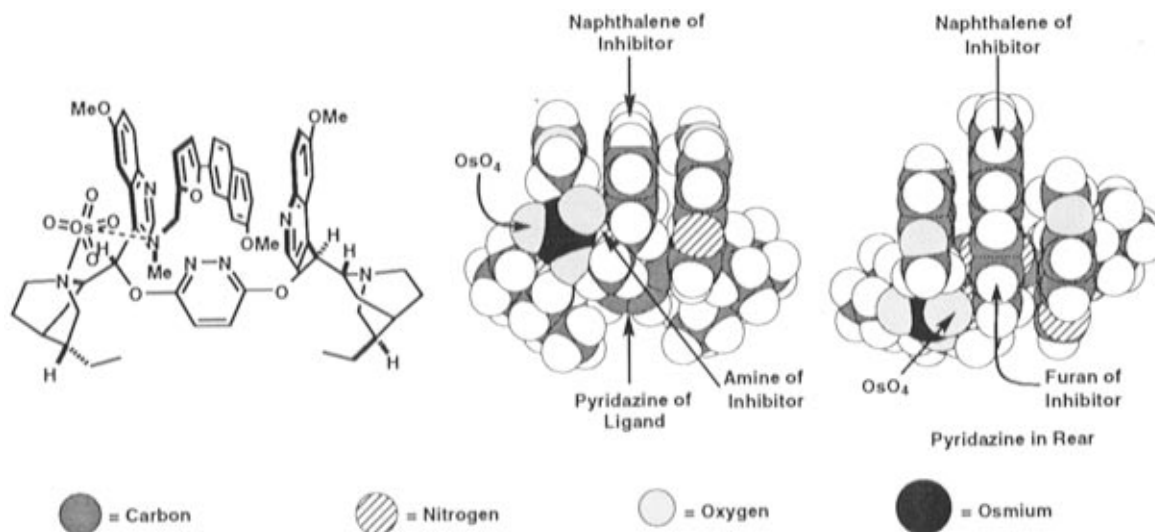


Figure 11. Three views of the proposed geometry for the complex between **19**, OsO_4 , and $(\text{DHQD})_2\text{PYDZ}$ ligand (**1**). The catalyst geometry was based on the X-ray crystal structure of $\mathbf{1}\cdot\text{CH}_3\text{I}$ with the following modifications: (a) the methyl group of the methiodide salt was replaced by OsO_4 with the eclipsed arrangement about the N–Os bond and the bond distances demonstrated from X-ray studies and (b) the H(8)–C(8)–C(9)–H(9) dihedral angle was adjusted to *ca.* 90° .

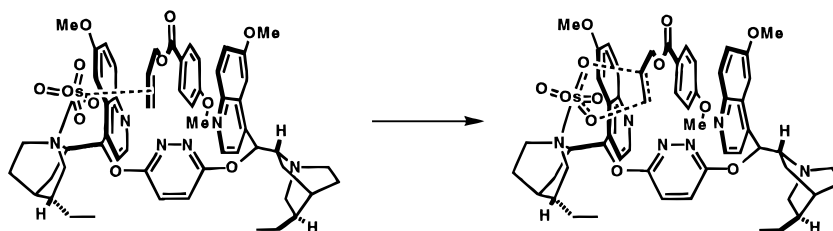


Figure 12. Stereoformula representation of the complex between allyl 4-methoxybenzoate (**2**) and the $(\text{DHQD})_2\text{PYDZ}\cdot\text{OsO}_4$ catalyst ($\mathbf{1}\cdot\text{OsO}_4$). The [3 + 2] cycloaddition reaction to produce the pentacoordinate osmate ester proceeds via rotation of the Os–N bond to the staggered Q·OsO₄ conformation with concurrent oxidation of the substrate double bond.

lene-2-methylamine (**14**) and 6-methoxynaphthalene-2-methanol (**15**) are considerably better inhibitors of catalyst activity than the corresponding methoxymethyl ether **16**. Moreover, inhibitory activity is sensitive to the length of the aromatic substituent of the inhibitor, as indicated by the better binding constants of the methoxynaphthylfurfurylamine **19** and alcohol **18** as compared to those of the corresponding naphthalene derivatives **14** and **15**.¹⁵ A comparison of the binding affinity of **19** with adamantylmethyl-*N*-methylamine (**20**) indicates 90-fold better binding activity for the former, as expected since the adamantyl group is too bulky to be accommodated in the binding pocket. Moreover, the presence of *unsaturated functionality* also enhances inhibitory activity. Thus, methyl 6-methoxynaphthyl-2-propenoate **17** exhibits inhibitory activity that is comparable to the best non-olefinic inhibitors.¹⁶ The dependence of effective inhibitory activity on the presence of both an extended aromatic group and an additional coordinating ligand suggests that two contact sites may be important for binding of these inhibitors. Indeed, each of the effective inhibitors shown in Table 3 possesses a hydroxyl, amine, or olefinic function which is capable of association with the Os(VIII) center of the catalyst as the aromatic group is bound within the U-shaped pocket, as can be seen by the examination of molecular models. Such two-site binding is illustrated for the case of **19** in Figure 11.

(15) Methoxy groups were incorporated into the design of aromatic inhibitors due to the enhanced solubility of these derivatives relative to the corresponding nonfunctionalized naphthalenes in the *tert*-butyl alcohol–water solvent system used for the dihydroxylation reaction.

(16) Inhibitors **17** and **18** were found to be partially oxidized by the $(\text{DHQD})_2\text{PYDZ}\cdot\text{OsO}_4$ catalyst (*ca.* 5–10% conversion) during the inhibitor assays.

The observation of two-site binding interactions in the inhibition studies suggests that the asymmetric dihydroxylation reaction itself involves rapid reversible formation of such a catalyst–substrate complex prior to transition state development. This complex would involve contacts between the olefinic π -orbital and the low-lying d-orbitals of Os(VIII) in addition to the hydrophobic or aryl–aryl interactions between an olefin substituent and the catalytic binding pocket that are crucial to high enantioselection in the asymmetric dihydroxylation. The proposed geometry of such a complex is indicated in Figure 12 for the asymmetric dihydroxylation of allyl 4-methoxybenzoate **2**. Thus, in the case of the bis-cinchona alkaloid catalyzed asymmetric dihydroxylation, complexation of the olefin with osmium tetroxide occurs simultaneously with binding of an olefinic substituent in the U-shaped binding pocket of the catalyst. Optimum olefin–Os(VIII) d- π contact is attained when the equatorial oxygen atoms of the complexed OsO_4 are eclipsed with the C–N bonds of the quinuclidine ring. Subsequent rotation of the OsO_4 unit about the Os–N bond relieves these eclipsing interactions and positions one axial and one equatorial oxygen proximal to the double bond as required for the five-membered [3 + 2] cycloaddition transition state and enantioselective production of the Os(VI) ester. This two-site binding interaction and enantioselective delivery of two oxygen atoms to the double bond of the substrate are shown in Figure 12. The enantioselective acceleration (selective acceleration of the pathway leading to the preferred enantiomer) of the dihydroxylation would then result from a combination of two factors: (1) favorable complexation which brings the two reactants together in the appropriate geometry, thereby providing a high effective concentration (entropic effect) and (2) a driving force due to

the subsequent Os–N bond rotation (from eclipsed to the more stable staggered geometry) which lowers the activation enthalpy. Dihydroxylation of the opposite olefin face is disfavored due to the fact that there is no suitable three-dimensional arrangement for simultaneous interaction of the substrate with osmium tetroxide and the catalyst binding pocket.

Conclusions

Kinetic studies on the OsO₄-promoted dihydroxylation of olefins using (DHQD)₂PYDZ (**1**) as catalyst have demonstrated Michaelis–Menten behavior and the intermediacy of a rapidly and reversibly formed complex of **1**·OsO₄·olefin prior to transition state development. There is a good correlation between stability of the initial complex (low *K_m* value) and the enantioselectivity of the dihydroxylation process. There is also a good correlation between the ability of various molecules to inhibit this oxidation and their structural capacity to coordinate to Os(VIII) while simultaneously fitting into the U-shaped binding pocket of the catalytic ligand. These results are fully consistent with a two-step oxidation mechanism involving (1) reversible formation of an olefin–Os(VIII) π -d complex and (2) slow rearrangement to the [3 + 2] cycloaddition transition state, as shown in Figure 12. The [3 + 2] cycloaddition transition state shown in figure 12, which has previously been discussed,^{3b–d,4} adequately explains all of the available experimental evidence, to the best of our knowledge.

A different mechanism involving [2 + 2] addition of the olefinic bond to complexed OsO₄ with interactions between the substrate and an L-shaped binding area has recently been proposed by Sharpless.¹⁷ A critical analysis of the [2 + 2] mechanism based on the results presented here and other data will appear in a forthcoming paper.

Experimental Section

General Methods. All moisture and air sensitive reactions were performed in oven or flame dried glassware equipped with rubber septa under a positive pressure of nitrogen or argon. When necessary, solvents and reagents were distilled prior to use and were transferred using a syringe or cannula. Reaction mixtures were magnetically stirred. Thin layer chromatography was performed on Merck precoated silica gel F-254 plates (0.25 mm). Concentration *in vacuo* was generally performed using a Büchi rotary evaporator. Flash column chromatography was performed on Baker 230–400 mesh silica gel. Melting points were determined using a Büchi oil immersion apparatus and are reported uncorrected for all crystalline products. All other products were isolated as clear oils. Optical rotations were determined using a Perkin-Elmer 241 polarimeter. Infrared spectra were recorded on a Nicolet 5ZDX FT-IR. Nuclear magnetic resonance spectra were measured with Bruker AM500, AM400, AM300, and AM250 instruments. Proton NMR spectra were obtained with CDCl₃ as solvent using the CHCl₃ signal as an internal standard (7.26 ppm). Carbon NMR spectra were recorded in ppm relative to the solvent signal: CDCl₃ (77.07 ppm). Mass spectra and high resolution mass spectra (HRMS) were recorded on JEOL Model AX-505 or SX-102 spectrometers and are reported in units of mass to charge (*m/e*). Chiralcel and Chiralpak HPLC columns were obtained from Daicel Chemical Industries, Ltd. Gas chromatographic analysis was performed using a Hewlett Packard 5890A gas chromatograph interfaced to a Hewlett Packard 3392A integrator. Separations were performed using a Sigma-Aldrich SA-1 capillary column (0.32 mm i.d. × 30 m) under the conditions indicated below.

General Conditions for Kinetic Experiments. Unless otherwise indicated, the following general procedure was used for the kinetic experiments. A stock oxidant solution was prepared by charging a 25

mL volumetric flask with K₂OsO₄ (4.6 mg, 0.013 mmol), K₃Fe(CN)₆ (2.47 g, 7.50 mmol), K₂CO₃ (1.04 g, 7.52 mmol) and diluting to the mark with deionized water. A stock solution of (DHQD)₂PYDZ ligand **1** was prepared by charging a 10 mL volumetric flask with **1** (7.3 mg, 0.01 mmol) and diluting to the mark with *tert*-butyl alcohol. A 10 mL round-bottom flask was charged with 1.00 mL of each of these stock solutions and was cooled to 0 °C with vigorous magnetic stirring. Since this mixture consisted of a solid phase of undissolved salts, a salt-containing aqueous phase, and an organic phase, all substrate and catalyst concentrations are based on the estimated volume of the organic phase as 50% of the total reaction volume or 1.0 mL. Thus, the above mixture is calculated to contain 1 mM (DHQD)₂PYDZ ligand **1** and 0.5 mM K₂OsO₄·2H₂O. A crystal of hydroquinone was added to solutions of the substituted styrenes to inhibit polymerization of the olefin. The appropriate amount of olefin solution (see below) was added, and aliquots were taken at recorded times according to the following procedure. Approximately 0.02 mL of the reaction mixture was withdrawn with a Pasteur pipette and was immediately introduced into a 0.5 mL test tube containing approximately 0.1 mL of saturated aqueous Na₂SO₃ solution and 0.2 mL of ethyl acetate. The resulting mixture was thoroughly agitated, and 0.003 mL of the organic layer was withdrawn and analyzed by gas chromatography. Reaction rates were followed by monitoring olefin concentration relative to that of an internal standard. For each aliquot, the ratio of integrated areas under the olefin and internal standard peaks were compared with that measured before the reaction and were scaled against the initial concentration of olefin. The initial ratio of peak areas for the single substrate and inhibitor studies was obtained by extrapolation of the linear plot of the ratio of areas versus total reaction time. In general, the calculated values agreed to within 5% of those measured from the initial olefin stock solutions.

Competitive Rate Experiments with Two Substrates. (a) Allyl 4-methoxybenzoate **2** vs allyl triisopropylsilyl ether **6**: A stock oxidant solution was prepared by charging a 25 mL volumetric flask with K₂OsO₄ (3.7 mg, 0.010 mmol), K₃Fe(CN)₆ (3.95 g, 12.0 mmol), K₂CO₃ (1.65 g, 12.0 mmol) and diluting to the mark with deionized water. A stock solution of (DHQD)₂PYDZ ligand **1** was prepared by charging a 10 mL volumetric flask with **1** (11.7 mg, 0.0161 mmol) and diluting to the mark with *tert*-butyl alcohol. A 10 mL round-bottom flask was charged with 1.00 mL of each of these stock solutions and was cooled to 0 °C with vigorous magnetic stirring. A mixture of **2** (0.042 mL, 46 mg, 0.24 mmol), **6** (0.061 mL, 52 mg, 0.24 mmol), and 0.05 mL of tetralin (added as an internal standard) was prepared, and 0.051 mL of this solution was added to the reaction mixture prepared above. Aliquots were taken and analyzed as indicated in the general procedure: GC conditions, injector temperature, 225 °C; detector temperature, 300 °C, FID detection, 120 °C isothermal oven, 1.1 mL/min carrier gas flow rate; retention times, **2** = 8.95 min; **6** = 2.84 min; tetralin = 2.11 min.

(b) **4-Vinylanisole 8** vs **Decene 10**. A stock oxidant solution was prepared by charging a 25 mL volumetric flask with K₂OsO₄ (3.7 mg, 0.010 mmol), K₃Fe(CN)₆ (3.95 g, 12.0 mmol), K₂CO₃ (1.65 g, 12.0 mmol) and diluting to the mark with deionized water. A stock solution of (DHQD)₂PYDZ ligand **1** was prepared by charging a 10 mL volumetric flask with **1** (11.7 mg, 0.016 mmol) and diluting to the mark with *tert*-butyl alcohol. A 10 mL round-bottom flask was charged with 1.00 mL of each of these stock solutions and was cooled to 0 °C with vigorous magnetic stirring. A mixture of **8** (0.032 mL, 32 mg, 0.24 mmol), **10** (0.045 mL, 34 mg, 0.24 mmol), and 0.03 mL of tetralin (added as an internal standard) was prepared, and 0.036 mL of this solution was added to the reaction mixture prepared above. Aliquots were taken and analyzed as indicated in the general procedure: GC conditions, injector temperature, 250 °C; detector temperature, 300 °C FID detection, 95 °C isothermal oven, 1.1 mL/min carrier gas flow rate; retention times, **8** = 3.12 min; **10** = 1.73 min; tetralin = 3.35 min.

(c) **Allyl Triisopropylsilyl Ether 6** vs **4-Vinylanisole 8**. A stock oxidant solution was prepared by charging a 25 mL volumetric flask with K₂OsO₄ (3.7 mg, 0.010 mmol), K₃Fe(CN)₆ (3.95 g, 12.0 mmol), K₂CO₃ (1.65 g, 12.0 mmol) and diluting to the mark with deionized water. A stock solution of (DHQD)₂PYDZ ligand **1** was prepared by charging a 10 mL volumetric flask with **1** (11.7 mg, 0.016 mmol) and

(17) (a) Norrby, P.-O.; Kolb, H. C.; Sharpless, K. B. *Organometallics* **1994**, *13*, 344. (b) Norrby, P.-O.; Kolb, H. C.; Sharpless, K. B. *J. Am. Chem. Soc.* **1994**, *116*, 8470. (c) Becker, H.; Ho, P. T.; Kolb, H. C.; Loren, S.; Norrby, P.-O.; Sharpless, K. B. *Tetrahedron Lett.* **1994**, *35*, 7315.

diluting to the mark with *tert*-butyl alcohol. A 10 mL round-bottom flask was charged with 1.00 mL of each of these stock solutions and was cooled to 0 °C with vigorous magnetic stirring. A mixture of **6** (0.061 mL, 52 mg, 0.24 mmol), **8** (0.032 mL, 32 mg, 0.24 mmol), and 0.03 mL of tetralin (added as an internal standard) was prepared, and 0.041 mL of this solution was added to the reaction mixture prepared above. Aliquots were taken and analyzed as indicated in the general procedure: GC conditions, injector temperature, 250 °C; detector temperature, 300 °C, FID detection, 115 °C isothermal oven, 1.1 mL/min carrier gas flow rate; retention times, **6** = 2.69 min; **8** = 1.80 min; tetralin = 1.92 min.

(d) **Styrene (7) vs 4-Vinylanisole (8)**. The asymmetric dihydroxylation reaction mixture was set up as described in the general procedure. A mixture of **7** (0.086 mL, 78 mg, 0.75 mmol), **8** (0.100 mL, 101 mg, 0.75 mmol), and 0.08 mL of tetralin (added as an internal standard) in a 1 mL volumetric flask was diluted to the mark with *tert*-butyl alcohol, and 0.053 mL of this solution was added to the reaction mixture prepared above. Aliquots were taken and analyzed as indicated in the general procedure: GC conditions, injector temperature, 250 °C, detector temperature, 300 °C, FID detection, 95 °C isothermal oven, 1.1 mL/min carrier gas flow rate; retention times, **7** = 1.43 min; **8** = 3.87 min; tetralin = 4.15 min.

(e) **Styrene (7) vs Decene (10)**. The asymmetric dihydroxylation reaction mixture was set up as described in the general procedure. A mixture of **7** (0.100 mL, 90.9 mg, 0.873 mmol), **10** (0.166 mL, 123 mg, 0.877 mmol), and 0.100 mL of tetralin (added as an internal standard) in a 1 mL volumetric flask was diluted to the mark with *tert*-butyl alcohol, and 0.046 mL of this solution was added to the reaction mixture prepared above. Aliquots were taken and analyzed as indicated in the general procedure: GC conditions, injector temperature, 250 °C, detector temperature, 300 °C, FID detection, 90 °C isothermal oven, 1.1 mL/min carrier gas flow rate; retention times, **7** = 1.55 min; **10** = 2.22 min; tetralin = 4.51 min.

(f) **Allyl Triisopropylsilyl Ether (6) vs Decene (10)**. The asymmetric dihydroxylation reaction mixture was set up as described in the general procedure. A mixture of **6** (0.200 mL, 168 mg, 0.785 mmol), **10** (0.148 mL, 110 mg, 0.782 mmol), and 0.150 mL of tetralin (added as an internal standard) in a 1 mL volumetric flask was diluted to the mark with *tert*-butyl alcohol, and 0.051 mL of this solution was added to the reaction mixture prepared above. Aliquots were taken and analyzed as indicated in the general procedure: GC conditions, injector temperature, 225 °C, detector temperature, 300 °C, FID detection, 120 °C isothermal oven, 1.1 mL/min carrier gas flow rate; retention times, **6** = 3.44 min; **10** = 1.55 min; tetralin = 2.47 min.

(g) **4-Vinylanisole (8) vs 4-Cyanostyrene (9)**.¹⁸ The asymmetric dihydroxylation reaction mixture was set up as described in the general procedure. A mixture of **8** (0.100 mL, 101 mg, 0.752 mmol), **9** (0.094 mL, 97 mg, 0.75 mmol), and 0.100 mL of tetralin (added as an internal standard) in a 1 mL volumetric flask was diluted to the mark with *tert*-butyl alcohol, and 0.053 mL of this solution was added to the reaction mixture prepared above. Aliquots were taken and analyzed as indicated in the general procedure: GC conditions, injector temperature, 250 °C, detector temperature, 300 °C, FID detection, 115 °C isothermal oven, 1.1 mL/min carrier gas flow rate; retention times, **8** = 2.10 min; **9** = 2.48 min; tetralin = 2.25 min.

Determination of the Michaelis–Menten Constants K_m and V_{max} . The catalytic asymmetric dihydroxylation reactions were carried out and analyzed according to the general procedure. Olefins were added as stock solutions prepared in *tert*-butyl alcohol containing the appropriate internal standard. The initial substrate concentrations are based on the estimated volume of 1 mL for the organic layer of the reaction. Initial velocities were measured to 10–30% conversion of the olefin. Values of K_m and V_{max} were measured from single, linear Lineweaver–Burk plots using established procedures. Gas chromatographic retention times are indicated below.

Allyl 4-Methoxybenzoate (2). Tetralin was used as the internal standard: GC conditions, injector temperature, 250 °C, detector temperature, 300 °C, FID detection, 130 °C isothermal oven, 0.45 mL/min carrier gas flow rate; retention times, **2** = 9.72 min; tetralin = 2.87 min.

Allyl Triisopropylsilyl Ether (6). Tetralin was used as the internal standard: GC conditions, injector temperature, 250 °C; detector

temperature, 300 °C, FID detection, 120 °C isothermal oven, 1.1 mL/min carrier gas flow rate; retention times, **2** = 3.33 min; tetralin = 2.47 min.

Styrene (7). Tetralin was used as the internal standard: GC conditions, injector temperature 250 °C; detector temperature 300 °C, FID detection, 90 °C isothermal oven, 0.45 mL/min carrier gas flow rate; retention times, **2** = 2.46 min; tetralin = 7.06 min.

4-Vinylanisole (8). Tetralin was used as the internal standard: GC conditions, injector temperature, 250 °C; detector temperature, 300 °C, FID detection, 115 °C isothermal oven, 1.1 mL/min carrier gas flow rate; retention times, **8** = 2.28 min; tetralin = 2.44 min.

4-Cyanostyrene (9). Tetralin was used as the internal standard: GC conditions, injector temperature, 250 °C; detector temperature, 300 °C, FID detection, 115 °C isothermal oven, 1.1 mL/min carrier gas flow rate; retention times, **9** = 2.27 min; tetralin = 2.05 min.

1-Decene (10). Tetralin was used as the internal standard: GC conditions, injector temperature, 250 °C; detector temperature, 300 °C, FID detection, 90 °C isothermal oven, 0.45 mL/min carrier gas flow rate; retention times, **10** = 3.23 min; tetralin = 6.52 min.

(E)-Methylcinnamate (11). The kinetic studies were carried out as described in the general Experimental Section, with the exception that 9.5 mg (0.10 mmol) of methanesulfonamide was added to each reaction prior to the addition of olefin to ensure rapid hydrolysis of the osmate ester intermediate. Tetralin was used as the internal standard: GC conditions, injector temperature, 250 °C; detector temperature 300 °C, FID detection, 120 °C isothermal oven, 1.1 mL/min carrier gas flow rate; retention times, **11** = 4.89 min; tetralin = 2.31 min.

4-Cyano-(E)-methylcinnamate (12). The kinetic studies were carried out as described in the general Experimental Section, with the exception that 9.5 mg (0.10 mmol) of methanesulfonamide was added to each reaction prior to the addition of olefin to ensure rapid hydrolysis of the osmate ester intermediate. Heptadecane was used as the internal standard: GC conditions, injector temperature, 250 °C; detector temperature, 300 °C, FID detection, 170 °C isothermal oven, 1.1 mL/min carrier gas flow rate; retention times, **12** = 3.56 min; heptadecane = 3.17 min.

Determination of the Inhibition Constants K_i for Inhibitors. The catalytic asymmetric dihydroxylation reactions were carried out and analyzed according to the general procedure. A 1 mL volumetric flask was charged with styrene (0.100 mL, 0.091 g, 0.874 mmol), 0.100 mL of tetralin, and one crystal of hydroquinone and was diluted to the mark with *tert*-butyl alcohol. Inhibitors were added as stock solutions in *tert*-butyl alcohol and were soluble in the dihydroxylation mixture at all concentrations used. The styrene stock solution (0.020 mL, 0.0175 mmol styrene) was added, and aliquots were taken and analyzed as described in the general Experimental Section. The inhibitor concentrations are based on the estimated volume of 1 mL for the organic layer of the reaction. Initial velocities were measured to 10–30% conversion of the olefin. Values of K_i were measured from single linear Dixon plots of $1/v$ vs $[I]$, where

$$K_i = K_m / (mV_{max}[S])$$

$$K_m = K_m \text{ for styrene} = 0.017 \text{ M}$$

$$V_{max} = V_{max} \text{ for styrene} = 1.3 \times 10^{-4} \text{ M/s}$$

$$[S] = \text{initial styrene concentration} = 0.0175 \text{ M}$$

$$m = \text{slope of the linear Dixon plot}$$

N-Methylnaphthalene-2-methylamine (14). To a suspension of lithium aluminum hydride (0.123 g, 3.24 mmol) in 50 mL of ether was added *N*-methyl-2-naphthalenecarboxamide (0.50 g, 2.7 mmol). The resulting mixture was stirred for 10 min at 23 °C and for 1.5 h at reflux. After cooling to 23 °C, 0.123 mL of water was slowly added, followed by 0.36 mL of 1 M NaOH and an additional 0.123 mL of water. The mixture was stirred for 20 min, and the precipitated solids were filtered and washed with 100 mL of ether. The filtrate was extracted into 1 M HCl until the aqueous extracts were acidic. The combined aqueous layers were basified with 3 M NaOH extracted into ethyl acetate (3 × 50 mL), and the combined organic layers were dried

over MgSO_4 and concentrated *in vacuo*, giving 0.42 g (91%) of **14** as a colorless solid: mp 83 °C; R_f 0.25 (20% methanol–chloroform–2% NH_4OH); FTIR (NaCl plate) 3053, 3022, 2932, 2871, 2842, 2789, 1602, 1509, 1473, 1443, 1124, 1101, 854, 816 cm^{-1} ; ^1H NMR (500 MHz, CDCl_3) δ 7.81 (m, 3H), 7.76 (m, 1H), 7.45 (m, 3H), 3.93 (s, 2H), 2.5 (s, 3H), 2.44 (bs, 1H) ppm; ^{13}C NMR (125 MHz, CDCl_3) δ 137.5, 133.4, 132.7, 128.0, 127.7, 127.6, 126.6, 126.0, 125.5, 56.0, 35.9 ppm; CIMS 172 $[\text{M} + \text{H}]^+$; HRMS calcd for $[\text{C}_{12}\text{H}_{13}\text{N}]^+$ 171.1048, found 171.1053.

6-Methoxynaphthalene-2-Methylmethoxymethyl Ether (16). To a suspension of hexane washed KH (0.044 g, 1.1 mmol) in 10 mL of THF was added 6-methoxynaphthalene-2-methanol¹⁹ (0.20 g, 1.1 mmol), and the resulting mixture was stirred for 20 min at 23 °C. Bromomethyl methyl ether (0.098 mL, 0.15 g, 1.2 mmol) was added, and the resulting light yellow suspension was stirred for 13 h at 23 °C. The mixture was cautiously diluted with 10 mL of water and extracted into ethyl acetate (3 \times 20 mL), and the combined organic layers were dried over Na_2SO_4 , filtered, and concentrated *in vacuo*. Purification of the crude material by silica gel chromatography (1:4 ethyl acetate–hexane) gave 0.11 g (45%) of **16** as a colorless solid: mp 49 °C; R_f 0.35 (1:9 ethyl acetate–hexane); FTIR (NaCl plate) 2939, 2907, 2883, 2841, 2824, 1635, 1609, 1484, 1391, 1267, 1195, 1149, 1101, 1045, 1031, 932, 857, 817 cm^{-1} ; ^1H NMR (300 MHz, CDCl_3) δ 7.74 (m, 3H), 7.44 (d, 1H, $J = 8.6$ Hz), 7.16 (m, 2H), 4.74 (s, 2H), 4.72 (s, 2H), 3.92 (s, 3H), 3.45 (s, 3H) ppm; ^{13}C NMR (125 MHz, CDCl_3) δ 157.8, 134.2, 133.0, 129.4, 128.8, 127.0, 126.7, 126.6, 118.9, 105.8, 95.7, 69.4, 55.4, 55.3 ppm; EIMS 232, 171, 128; HRMS calcd for $\text{C}_{14}\text{H}_{16}\text{O}_3$ 232.1099, found 232.1096.

2-Furanmethyl tert-Butyldimethylsilyl Ether. To a solution of 2-furanmethanol (0.50 g, 5.1 mmol) in 5 mL of DMF was added imidazole (0.36 g, 5.3 mmol) and *tert*-butyldimethylsilylchloride (0.80 g, 5.3 mmol), and the resulting mixture was stirred for 30 min at 23 °C. The mixture was diluted with 100 mL of ether, washed with water (3 \times 50 mL) and brine (1 \times 50 mL), dried over MgSO_4 , and concentrated *in vacuo*, giving 1.05 g (97%) of 2-furanmethyl *tert*-butyldimethylsilyl ether as a colorless oil: R_f 0.65 (1:30 ethyl acetate–hexane); FTIR (NaCl plate) 2957, 2930, 2886, 2858, 1473, 1256, 1224, 1151, 1087, 1075, 1014, 919, 838 cm^{-1} ; ^1H NMR (400 MHz, CDCl_3) δ 7.37 (dd, 1H, $J = 0.7, 1.9$ Hz), 6.32 (dd, 1H, $J = 1.9, 3.0$ Hz), 6.22 (d, 1H, $J = 3.1$ Hz), 4.65 (s, 2H), 0.91 (s, 9H), 0.09 (s, 6H) ppm; ^{13}C NMR (100 MHz, CDCl_3) δ 154.3, 142.0, 110.2, 107.2, 58.2, 25.9, 18.5, –5.2 ppm.

5-(6-Methoxy- β -naphthyl)-2-furanmethanol (18). To a solution of 2-furanmethyl *tert*-butyldimethylsilyl ether (0.75 g, 3.5 mmol) in 4 mL of THF at 0 °C was added 1.4 mL of *n*-BuLi, and the mixture was stirred for 2 h at 0 °C. A solution of ZnCl_2 (0.436 g in 3.4 mL of THF) was added, and the resulting mixture was stirred for 15 min at 0 °C. 6-Methoxy-2-iodonaphthalene²⁰ (0.67 g, 2.35 mmol, in 4 mL of THF) was added, followed by $\text{PdCl}_2(\text{PPh}_3)_2$ (0.05 g, 0.07 mmol), and the mixture was stirred for 12 h at 23 °C. After diluting with 20 mL of water, the mixture was extracted into ethyl acetate (3 \times 20 mL), and the combined organic layers were dried over Na_2SO_4 , filtered, and concentrated *in vacuo*. The crude residue was taken up in 35 mL of THF, and 1.7 mL of 1 M TBAF in THF (5% water) was added. After stirring for 20 min at 23 °C, water (20 mL) was added, and the mixture was extracted into ethyl acetate (3 \times 50 mL). The combined organic layers were dried over Na_2SO_4 , filtered and concentrated *in vacuo*. Purification by radial chromatography (1:4 ethyl acetate–hexane, followed by 2:1 ethyl acetate–hexane, 4 mm plate) gave 0.30 g of **18** as a colorless solid (50%): mp 144 °C; R_f 0.33 (1:1 ethyl acetate–hexane); FTIR (NaCl plate) 3334, 2964, 2936, 2908, 2843, 1253, 1208, 1164, 1022, 1005, 860 cm^{-1} ; ^1H NMR (400 MHz, CDCl_3) δ 8.08 (s, 1H), 7.75 (d, 1H, $J = 8.9$ Hz), 7.73 (d, 2H, $J = 1.1$ Hz), 7.15 (dd, 1H,

$J = 2.5, 8.9$ Hz), 7.12 (d, 1H, $J = 2.5$ Hz), 6.66 (d, 1H, $J = 3.3$ Hz), 6.41 (d, 1H, $J = 3.3$ Hz), 4.71 (d, 2H, $J = 6.1$ Hz), 3.93 (s, 3H), 1.79 (t, 1H, $J = 6.1$ Hz) ppm; ^{13}C NMR (100 MHz, CDCl_3) δ 154.3, 153.4, 133.9, 129.7, 128.9, 127.1, 126.0, 122.8, 122.2, 119.3, 110.1, 105.9, 105.5, 57.7, 55.3 ppm; EIMS 254 $[\text{M}]^+$, 237; HRMS calcd for $\text{C}_{16}\text{H}_{14}\text{O}_3$ 254.0943, found 254.0951.

5-(6-Methoxynaphthyl)furan-2-carboxaldehyde. To a solution of 5-(6-methoxynaphthyl)furan-2-methanol (0.20 g, 1.2 mmol) in 100 mL of CH_2Cl_2 was added MnO_2 (1.03 g, 11.8 mmol), and the suspension was stirred for 1 h at 23 °C. Filtration of the mixture through a pad of Celite and concentration gave 0.18 g (90%) of 5-(6-methoxynaphthyl)furan-2-carboxaldehyde as a yellow solid: mp 139 °C; R_f 0.47 (1:1 ethyl acetate–hexane); FTIR (NaCl plate) 1662, 1393, 1268, 1251, 1206, 1166, 1029, 942, 891, 858, 814 cm^{-1} ; ^1H NMR (400 MHz, CDCl_3) δ 9.66 (s, 1H), 8.29 (s, 1H), 7.80 (m, 3H), 7.35 (d, 1H, $J = 3.7$ Hz), 7.20 (dd, 1H, $J = 2.5, 8.9$ Hz), 7.14 (d, 1H, $J = 2.3$ Hz), 6.90 (d, 1H, $J = 3.7$ Hz), 3.94 (s, 3H) ppm; ^{13}C NMR (100 MHz, CDCl_3) δ 177.0, 159.9, 158.8, 151.9, 135.1, 130.1, 128.7, 127.5, 124.8, 124.1, 123.1, 119.8, 107.4, 105.9, 55.4 ppm; EIMS 252 $[\text{M}]^+$; HRMS calcd for $\text{C}_{16}\text{H}_{12}\text{O}_3$, 252.0786, found 252.0788.

***N*-Methyl-5-(6-methoxy- β -naphthyl)-2-furanmethylamine (19).** To a suspension of 3 Å molecular sieves (1.5 g) in 20 mL of methanol was added methylamine hydrochloride (2.4 g, 35 mmol, flame dried). Methylamine was bubbled in from a solution of methylamine hydrochloride (3.0 g, 44 mmol) in 4 mL of 50% aqueous KOH. 5-(6-Methoxy- β -naphthyl)furan-2-carboxaldehyde (0.18 g, 0.70 mmol) was added, and the resulting mixture was stirred for 30 min at 23 °C. NaCNBH_3 (0.047 g, 0.75 mmol) was added, and the mixture was stirred for 10 h at 23 °C. The mixture was filtered, and the solids were washed with 10 mL of water and 20 mL of ethyl acetate. After concentration *in vacuo*, the aqueous residue was taken up in 50 mL of saturated aqueous K_2CO_3 and extracted into ethyl acetate (3 \times 50 mL). The combined organic layers were dried over Na_2SO_4 and concentrated *in vacuo*. Purification of the crude product by silica gel chromatography (3% methanol–chloroform–0.3% NH_4OH) gave 0.14 g (73%) of **19** as a colorless solid: mp 88 °C; R_f 0.31 (10% methanol–chloroform–1% NH_4OH); FTIR (NaCl plate) 2998, 2952, 2840, 2794, 1630, 1616, 1595, 1500, 1463, 1391, 1271, 1254, 1204, 1164, 1031, 853 cm^{-1} ; ^1H NMR (400 MHz, CDCl_3) δ 8.06 (s, 1H), 7.74 (d, 1H, $J = 7.1$ Hz), 7.16 (m, 3H), 7.14 (dd, 1H, $J = 1.9, 7.1$ Hz), 7.11 (d, 1H, $J = 1.6$ Hz), 6.63 (d, 1H, $J = 2.5$ Hz), 6.30 (d, 1H, $J = 2.5$ Hz), 3.92 (s, 3H), 3.84 (s, 2H), 2.51 (s, 3H) ppm; ^{13}C NMR (100 MHz, CDCl_3) δ 157.7, 153.6, 153.3, 132.7, 129.6, 129.0, 127.1, 126.9, 122.8, 121.8, 119.2, 109.3, 105.9, 105.4, 55.3, 48.2, 35.7 ppm; EIMS 267 $[\text{M}]^+$, 237 $[\text{M} - \text{CH}_3 - \text{NH}]^+$; HRMS calcd for $\text{C}_{17}\text{H}_{17}\text{NO}_2$ 267.1259, found 267.1259.

***N*-Methyl-[1-adamantylmethyl]carboxamide.** To a solution of 1-adamantanecarboxylic acid (1.0 g, 5.6 mmol) (Aldrich) in 50 mL of CH_2Cl_2 was added oxalyl chloride (0.50 mL, 0.72 g, 5.7 mmol) and 3 drops of DMF. The mixture was stirred for 1 h at 23 °C, after which point gas evolution ceased. The mixture was cooled to 0 °C, and methylamine was bubbled in over 20 min. The reaction was monitored by IR spectroscopy. Upon complete consumption of the acid chloride, the mixture was diluted with 100 mL of ethyl acetate, washed with 20 mL of 1 M HCl, 20 mL of saturated aqueous NaHCO_3 , dried with MgSO_4 , and concentrated *in vacuo*, giving 1.03 g (96%) of *N*-methyl-[1-adamantylmethyl]carboxamide as a colorless solid: mp 137 °C; R_f 0.13 (1:1 ethyl acetate–hexane); FTIR (NaCl plate) 3308, 2925, 2902, 2849, 1630, 1542, 1449, 1401, 1344, 1328, 1288, 1237, 1151 cm^{-1} ; ^1H NMR (400 MHz, CDCl_3) δ 7.5 (b, 1H, rotamer A), 5.6 (b, 1H, rotamer B), 2.90 (d, 3H, $J = 5.22$ Hz, rotamer A), 2.78 (d, 3H, $J = 4.7$ Hz, rotamer B), 2.03 (s, 3H), 1.84 (s, 6H), 1.70 (m, 6H) ppm; ^{13}C NMR (100 MHz, CDCl_3) δ 178.5, 40.6, 39.2, 36.5, 28.1, 26.2, 26.1 ppm (two rotamers); CIMS 387 $[2\text{M} + \text{H}]^+$, 194 $[\text{M} + \text{H}]^+$; HRMS calcd for $\text{C}_{12}\text{H}_{19}\text{NO}$ 194.1545, found 194.1541.

***N*-Methyl-[1-adamantylmethyl]amine (20).** To a solution of *N*-methyl-1-adamantylmethylcarboxamide (0.30 g, 1.6 mmol) in 30 mL of THF was added lithium aluminum hydride (0.070 g, 1.9 mmol), and the mixture was stirred for 1.5 h at reflux. An additional 0.07 g of lithium aluminum hydride was added, and the mixture was stirred at reflux for 5 h. The mixture was cooled to 23 °C, and 0.14 mL of water was added slowly, followed by 0.42 mL of 1 M NaOH and 0.14

(18) Broos, R.; Anteunis, M. *Synth. Commun.* **1976**, *6*, 53.

(19) Eriguchi, A.; Takegoshi, T. *Chem. Pharm. Bull.* **1982**, *30*, 428.

(20) Brown, J. M.; Cook, S. J.; Khan, R. *Tetrahedron* **1986**, *42*, 5105.

(21) Neilson, D. G.; Zakir, U.; Scrimgeour, C. M. *J. Chem. Soc. C.* **1971**, 898.

(22) Wang, Z.-M.; Kolb, H. C.; Sharpless, K. B. *J. Org. Chem.* **1994**, *59*, 5104.

(23) (a) Pac, C.; Miyauchi, Y.; Ishitani, O.; Ihama, M.; Yasuda, M.; Sakurai, H. *J. Org. Chem.* **1984**, *49*, 26. (b) Davies, W.; Holmes, B. M.; Kefford, J. F. *J. Chem. Soc.* **1939**, 357.

mL of water. The mixture was filtered, and the solids were washed with 50 mL of ether. The filtrate was concentrated *in vacuo*, the residue was dissolved in 10 mL of ether. HCl was slowly bubbled in over 10 min, and the precipitated HCl salt was collected and washed with ether. The solids were partitioned between 20 mL of ether and 10 mL of 1 M NaOH. The aqueous layer was extracted with ether (3 × 50 mL), and the combined organic layers were dried over MgSO₄ and concentrated *in vacuo*, giving 0.20 g (72%) of **20** as a colorless solid: mp 68 °C; *R*_f 0.46 (20% methanol–chloroform–2% NH₄OH); FTIR (NaCl plate) 2962, 2901, 2846, 2811, 2784, 1472, 1458, 1160, 1124, 1095, 987 cm⁻¹; ¹H NMR (250 MHz, CDCl₃) δ 2.43 (s, 3H), 2.22 (s, 2H), 1.96 (bs, 3H), 1.65 (m, 7H), 1.53 (s, 6H) ppm; ¹³C NMR (100 MHz, CDCl₃) δ 65.6, 40.9, 37.7, 37.2, 33.3, 28.5 ppm; CIMS 197 [M + NH₄]⁺, 180 [M + H]⁺; HRMS calcd for C₁₂H₂₁N 179.1674, found 179.1678.

General Procedure for Catalytic Asymmetric Dihydroxylation.

A solution of K₂CO₃ (3.00 equiv), K₃Fe(CN)₆ (3.00 equiv), K₂OsO₄·2H₂O (0.001 to 0.01 equiv), (DHQD)₂PYDZ (0.01 equiv), and CH₃SO₂NH₂ (only for 1,2-disubstituted and trisubstituted olefins, 1.00 equiv) in *tert*-butyl alcohol–water 1:1 was cooled to 0 °C. The resulting suspension was treated with the corresponding olefin (0.1 M with respect to total reaction volume). The mixture was stirred for the indicated time and was quenched by addition of Na₂SO₃ (12 equiv). The mixture was stirred for 5 min, warmed to 23 °C over 5 min, and partitioned between ethyl acetate and minimal water. The organic extract was washed twice with brine, dried with Na₂SO₄, and concentrated *in vacuo*. The residue was filtered through a silica gel plug, eluting with 2:1 ethyl acetate–hexane. The filtrate was concentrated *in vacuo* to afford the indicated yield of product.

Asymmetric Dihydroxylation of 4-Vinylanisole (8). Asymmetric dihydroxylation with 1 mol % of the (DHQD)₂PYDZ ligand **1** and 0.2 mol % of K₂OsO₄·2H₂O on 4-vinylanisole **8** (0.159 g, 1.19 mmol) according to the above general procedure gave 0.200 g (97%) of the corresponding diol as a colorless solid of 97% ee (determined by ¹H NMR integration of the corresponding bis-MTPA ester derivative (minor: 6.43 ppm, major: 6.32 ppm) mp 90–91 °C; [α]_D²³ –33° [c 0.42, EtOH], lit. –35° [EtOH]).²¹

Asymmetric Dihydroxylation of 4-Cyanostyrene (9). Asymmetric dihydroxylation according to the above general procedure using the (DHQD)₂PYDZ ligand **1** (1 mol %) and K₂OsO₄·2H₂O (0.1 mol %) on 0.040 g (0.31 mmol) of olefin²¹ at 0 °C for 18 h gave 0.046 g (92%) yield of the corresponding diol as a colorless solid of 97% ee (determined by ¹H NMR integration of the corresponding bis-MTPA ester derivative (major: 6.18 ppm, minor: 6.25 ppm)): mp 73 °C; *R*_f 0.22 (2:1 ethyl acetate–hexane); [α]_D²³ –23° [c 0.52, EtOH]; FTIR (NaCl plate): 3700–3200, 2930, 2878, 2231, 1610, 1407, 1082, 1058, 1035, 847 cm⁻¹; ¹H NMR (400 MHz, CDCl₃) δ 7.62 (d, 2H, *J* = 8.1 Hz), 7.47 (d, 2H, *J* = 8.1 Hz), 4.86 (dd, 1H, *J* = 3.4, 8.0 Hz), 3.78 (dd, 1H, *J* = 3.4, 11.3 Hz), 3.58 (dd, 1H, *J* = 8.0, 11.3 Hz), 3.3–2.3 (bs, 2H) ppm; ¹³C NMR (100 MHz, CDCl₃) δ 145.9, 132.2, 126.7, 118.6, 111.4, 73.8, 67.6 ppm; EIMS 163 [M]⁺; HRMS calcd for [C₉H₇NO₂]⁺ 163.0633, found 163.0638.

Asymmetric Dihydroxylation of (*E*)-Methylcinnamate (11). Asymmetric dihydroxylation according to the above general procedure using the (DHQD)₂PYDZ ligand **1** (1 mol %), K₂OsO₄·2H₂O (1 mol %), and 0.92 mmol of methanesulfonamide on 0.149 g (0.92 mmol) of **11**

at 0 °C for 96 h gave 0.135 g (75%) yield of the corresponding diol as a colorless solid of >98% ee (determined by ¹H NMR integration of the corresponding bis-MTPA ester derivative (minor: 6.55 ppm, major: 5.50 ppm)): mp 83–84 °C; *R*_f 0.35 (1:1 ethyl acetate–hexane); [α]_D²³ –6.3° [c 1.4, EtOH] (lit. +3.4° [c 1.19, EtOH]).²²

Asymmetric Dihydroxylation of 4-Cyano-(*E*)-methylcinnamate (12). Asymmetric dihydroxylation according to the above general procedure using the (DHQD)₂PYDZ ligand **1** (1 mol %), K₂OsO₄·2H₂O (1 mol %), and 0.31 mmol of methanesulfonamide on 0.057 g (0.31 mmol) of olefin²³ at 0 °C for 96 h gave 0.056 g (83%) yield of the corresponding diol as a colorless solid of >98% ee (determined by ¹H NMR integration of the corresponding bis-MTPA ester derivative (major: 6.5 ppm, minor: 6.4 ppm)): mp 133 °C; *R*_f 0.30 (2:1 ethyl acetate–hexane); [α]_D²³ –27° [c 0.45, EtOH]; FTIR (KBr pellet) 3340, 2229, 1742, 1438, 1272, 1215, 1111, 1058 cm⁻¹; ¹H NMR (400 MHz, CDCl₃) δ 7.67 (d, 2H, *J* = 8.3 Hz), 7.53 (d, 2H, *J* = 8.2 Hz), 5.09 (dd, 1H, *J* = 2.3, 7.4 Hz), 4.37 (dd, 1H, *J* = 2.6, 4.9 Hz), 3.85 (s, 3H), 3.15 (d, 1H, *J* = 5.2 Hz), 2.83 (d, 1H, *J* = 7.6 Hz) ppm; ¹³C NMR (100 MHz, CDCl₃) δ 172.6, 145.3, 132.2, 127.0, 118.6, 111.9, 74.1, 73.6, 53.2 ppm; CIMS 239 [M + NH₄]⁺; HRMS calcd for [C₁₁H₁₁NO₄ + NH₄]⁺ 239.1032, found 239.1037.

Asymmetric Dihydroxylation of Methyl-(6-methoxynaphthyl)-2-propenoate (17). Asymmetric dihydroxylation with 1 mol % (DHQD)₂PYDZ ligand **1** and 0.1 mol % of K₂OsO₄·2H₂O on methyl-(6-methoxynaphthyl)-2-propenoate **17** (0.02 g, 0.083 mmol) according to the above general procedure gave 0.015 g (66%) of the corresponding diol as a colorless solid of 97% ee (determined by chiral HPLC: Chiralcel OJ column, 25% 2-propanol–hexane, 1 mL/min, 254 nm detection, 23 °C): retention times, 29 min (major), 40 min (minor); mp 146 °C; *R*_f 0.22 (1:1 ethyl acetate–hexane); [α]_D²³ +11.2° [c 0.42, EtOH]; FTIR (NaCl plate) 3509, 2961, 2938, 1722, 1605, 1267, 1222, 1171, 1122, 1072, 1030, 855 cm⁻¹; ¹H NMR (500 MHz, CDCl₃) δ 7.97 (d, 1H, *J* = 1.5 Hz), 7.74 (t, 2H, *J* = 8.7 Hz), 7.61 (dd, 1H, *J* = 1.9, 8.7 Hz), 7.16 (dd, 1H, *J* = 2.4, 8.9 Hz), 7.12 (d, 1H, *J* = 2.4 Hz), 4.36 (t, 1H, *J* = 10.0 Hz), 4.13 (s, 1H), 3.92 (s, 3H), 3.86 (s, 3H), 3.83 (m, 1H), 2.47 (bs, 1H) ppm; ¹³C NMR (100 MHz, CDCl₃) δ 174.3, 158.1, 134.2, 133.1, 129.8, 128.5, 127.0, 124.5, 123.5, 119.2, 105.4, 79.7, 68.2, 55.3, 53.5 ppm; EIMS 276 [M]⁺, 245 [M – CH₃O]⁺, 217 [M – CH₃CO₂]⁺; HRMS calcd for C₁₅H₁₆O₅ 276.0998, found 276.0993.

Acknowledgment. This research was supported by an NSF Fellowship to M.C.N. and an NSF grant to E.J.C. We are grateful to Dr. Douglas Burdi for assistance with the stopped flow experiments.

Supporting Information Available: Figures showing Lineweaver–Burk plots for the catalytic asymmetric dihydroxylation of **2** and **6–12** and Dixon plots for the inhibition of the catalytic asymmetric dihydroxylation of **7** by **14–20** (16 pages). This material is contained in many libraries on microfiche, immediately follows this article in the microfilm version of the journal, can be ordered from the ACS, and can be downloaded from the Internet; see any current masthead page for ordering information and Internet access instructions.

JA952567Z